



HAL
open science

Transport of finite chains with free ends through thin channels

Christophe Coste, Michel Saint-Jean

► **To cite this version:**

Christophe Coste, Michel Saint-Jean. Transport of finite chains with free ends through thin channels. International Journal of Modern Physics B, 2021, 35 (6), pp.2150084. 10.1142/S0217979221500843 . hal-03457374

HAL Id: hal-03457374

<https://hal.science/hal-03457374>

Submitted on 30 Nov 2021

HAL is a multi-disciplinary open access archive for the deposit and dissemination of scientific research documents, whether they are published or not. The documents may come from teaching and research institutions in France or abroad, or from public or private research centers.

L'archive ouverte pluridisciplinaire **HAL**, est destinée au dépôt et à la diffusion de documents scientifiques de niveau recherche, publiés ou non, émanant des établissements d'enseignement et de recherche français ou étrangers, des laboratoires publics ou privés.

Transport of finite chains with free ends through thin channels

Christophe Coste and Michel Saint Jean

Laboratoire "Matière et Systèmes Complexes" (MSC), UMR 7057 CNRS,

Université Paris–Diderot (Paris 7), 75205 Paris Cedex 13, France

(Dated: November 28, 2020)

Abstract

We describe the transport of a finite chain of N identical particles in a thermal bath, through thin channels that forbid any crossing with a conceptually and technically simple method, that is neither restricted to the thermodynamic limit (infinite systems with finite density) nor to overdamped systems. We obtain analytically the mean squared displacement of each particle. Regardless of the damping, we identify a *correlated regime* for which chain transport is dominated by the correlations between individual particles. At large damping, the mean squared displacement evidences the typical single file behavior, with a time dependence that scales as $t^{1/2}$. At small damping, the correlated regime is rather described by a diffusion-like behavior, with a diffusivity which is neither the individual particle diffusivity nor the Fickian diffusivity of the chain as a whole. We emphasize that, for a chain with free ends, the fluctuations of the chain ends are larger by a factor two than the fluctuations of its center. This effect is observed whatever the damping γ , but the duration of this fluctuations enhancement is found to scale as N for low damping and as $N^2\gamma$ for high damping. We discuss the relevance of this model to the transport of actual systems in confined geometries.

PACS :

05.40.-a Fluctuation phenomena, random processes, noise, and Brownian motion

66.10.cg Mass diffusion, including self-diffusion, mutual diffusion, tracer diffusion, etc.

I. INTRODUCTION

Many physical systems may be described as a chain of interacting particles in a confined geometry, such that any crossing between particles is forbidden. In actual configurations, the typical size of the particles, hence of the confining device, extends on more than four orders of magnitudes, from nanometers for molecules up to several microns for colloidal particles. Relevant systems include intracellular transport of macromolecules [1, 2], molecular chains in microporous materials [3–6], ions in electrostatic traps [7], vortices in layered superconductor films [8–10] or colloids in microsized channels [11–15].

In these confined systems, the particles are submitted to a thermal bath that induces their diffusive transport. The lack of crossing between particles of the file induces strong correlations which results in a very specific sub-diffusive behavior, called single file diffusion (SFD). In this article, we study this peculiar diffusion for a finite chain with free ends. Obviously, in such systems the particle dynamics depend on their position in the file and the relevant transport coefficients differs from one particle to another. In order to describe quantitatively these effects, we calculate the mean squared displacement (MSD) of the i -th particle, $\langle \Delta x_i^2(t) \rangle$ as a function of the time t , where x_i is the position of the i -th tagged particle and where $\langle \cdot \rangle$ means ensemble averaging.

In infinite systems or in finite systems with periodic boundary conditions, all particles are equivalent and therefore their MSD is independent of their index i . In the thermodynamic limit (infinite systems with finite density), the SFD is evidenced by a scaling law $\langle \Delta x^2(t) \rangle = F\sqrt{t}$ where the prefactor F is customarily called the mobility. The mobility has been calculated, for hard core (zero range) interactions between the particles [16–19], and more recently for more realistic finite range interactions [20–22]. This behavior is still relevant for finite systems with periodic boundary conditions, even for systems of moderate size [7–15]. However, in this case, the SFD regime is followed by a Fickian free diffusion of the whole system considered as an effective particle. Explicit expressions of the diffusive transport coefficients and of the crossover times between the different regimes have been obtained [22].

In finite systems with free ends, the MSD calculation requires to take into account the particle position. This model is described in Sec. II. The analytical calculations are systematically compared to numerical simulations in Sec. III, for several values of the damping and of the chain length. In particular, we compare the motion of a particle at one extremity to

the motion of a particle at the center. In the conclusion, Sec. IV, we summarize our results and discuss their relevance to the description of actual systems.

II. DIFFUSION OF CHAIN WITH FREE ENDS

In order to calculate the MSD of a given particle, we describe its displacement as a superposition of vibrational eigenmodes of the chain, that explicitly depends on the position of the particle in the file. This is particularly convenient because the eigenmodes are uncorrelated, so that the MSD of each particle is explicitly given by a weighted sum of the MSD of the eigenmodes, where the weighting factors are given by the superposition. Moreover, this MSD is readily calculated because each eigenmode behaves as a fictitious particle submitted to a thermal bath, put in a harmonic well characterized by the relevant eigenfrequency.

A. Equations of motion

We consider N identical particles of mass m , ordered along a line. Their equilibrium positions are supposed to be equidistant from d (the density is $\rho = 1/d$). Assuming the stability of the system, the motion of the n -th particle is a small perturbation y_n around its equilibrium position $(n-1)d$ in the reference frame of the chain center of mass. When the chain is disturbed, the n -th particle is at position $x_n = (n-1)d + y_n$ for $1 \leq n \leq N$. We assume nearest neighbours interactions described by a potential $U(r)$, so that the distance d is such that $U'(d) \equiv dU/dr|_{r=d} = 0$. Therefore, up to the second order in the small quantities $(y_{n+1} - y_n)/d$, the potential energy of the chain is

$$U_{tot} = NU(d) + \frac{U''(d)}{2} \sum_{n=1}^N (y_{n+1} - y_n)^2. \quad (1)$$

The particles are submitted to a thermal bath at temperature T , which is described in the Langevin equation formalism. The n -th particle is submitted to a friction force $-m\gamma\dot{y}_n$, where γ is the damping coefficient and to a stochastic force $\mu_n(t)$. This random force has the statistical properties of a white gaussian noise (we do not consider in this paper the case of non-Markovian chains [23–25]), and we assume statistically independent forces on each particle.

The variables may be rescaled in the following way :

$$\tilde{y} \equiv y/d, \quad \tilde{t} = t\sqrt{U''(d)/m} \equiv \Omega t, \quad \Gamma = \gamma/\Omega, \quad \tilde{T} \equiv \frac{k_B T}{m\Omega^2 d^2}, \quad \tilde{\mu}_n(t) = \frac{\mu_n(t)}{md\Omega^2}. \quad (2)$$

From now on, we drop the tildes $\tilde{}$ and use these dimensionless variables.

The equations of motion therefore read

$$\begin{cases} \ddot{y}_1 + \Gamma \dot{y}_1 = y_2 - y_1 + \mu_1(t), \\ \ddot{y}_n + \Gamma \dot{y}_n = y_{n+1} + y_{n-1} - 2y_n + \mu_n(t), & (1 < n < N) \\ \ddot{y}_N + \Gamma \dot{y}_N = -(y_N - y_{N-1}) + \mu_N(t). \end{cases} \quad (3)$$

In dimensionless units, the stochastic forces are therefore such that

$$\langle \mu_n(t) \rangle = 0, \quad \langle \mu_n(t) \mu_p(t') \rangle = 2T\Gamma \delta_{np} \delta(t - t'). \quad (4)$$

The system (3) may be written

$$\mathcal{L}[y_n] = S_{np} y_p + \mu_n(t), \quad (5)$$

where summation is implicit on repeated indices that run from 1 to N , where we define the linear differential operator

$$\mathcal{L}[\cdot] \equiv \frac{d^2}{dt^2} + \Gamma \frac{d}{dt}, \quad (6)$$

and where we define the $N \times N$ dynamic matrix $\underline{\underline{S}}$,

$$\underline{\underline{S}} = \begin{pmatrix} -1 & 1 & 0 & 0 & \dots & 0 & 0 \\ 1 & -2 & 1 & 0 & \dots & 0 & 0 \\ \dots & \dots & \dots & \dots & \dots & \dots & \dots \\ 0 & 0 & \dots & 0 & 1 & -2 & 1 \\ 0 & 0 & 0 & \dots & 0 & 1 & -1 \end{pmatrix}. \quad (7)$$

B. Diagonalization of the dynamic matrix

The eigenvalues of this real symmetric matrix are $-\omega_s^2$ [26],

$$\omega_s = 2 \sin \frac{(s-1)\pi}{2N}, \quad (8)$$

with s an integer such that $1 \leq s \leq N$. The first frequency vanishes, $\omega_1 = 0$, and the corresponding eigenvector \mathbf{U}_1 describes a uniform motion of the chain. This mode traces

back to the translational invariance of the system, which implies that a vanishing energy is required to move the chain as a whole.

The eigenvectors \mathbf{U}_s have been calculated in Ref. [27]. We obtain an orthonormal basis that reads

$$U_1(n) = \frac{1}{\sqrt{N}}, \quad U_s(n) = \sqrt{\frac{2}{N}} \cos \frac{(s-1)(2n-1)\pi}{2N} \quad \text{for } s \geq 2. \quad (9)$$

This is obvious for \mathbf{U}_1 . For $s \geq 2$, let $\alpha = (s-1)\pi/N$. We get

$$\begin{aligned} \sum_{n=1}^N \cos^2(2n-1) \frac{\alpha}{2} &= \sum_{n=1}^N \left(\cos n\alpha \cos \frac{\alpha}{2} + \sin n\alpha \sin \frac{\alpha}{2} \right)^2 \\ &= \cos^2 \frac{\alpha}{2} \sum_{n=1}^N \cos^2 n\alpha + \sin^2 \frac{\alpha}{2} \sum_{n=1}^N \sin^2 n\alpha + \sin \frac{\alpha}{2} \cos \frac{\alpha}{2} \sum_{n=1}^N \sin 2n\alpha = \frac{N}{2}, \end{aligned}$$

where the last equality is given by known identities (see [28], formulae 1.351.1, 1.351.2 and 1.342.1).

C. Projection onto the eigenmodes

Let us now project the particles displacements onto the eigenvectors basis,

$$y_n(t) = Y_s(t)U_s(n), \quad (10)$$

where $Y_s(t)$ is a time dependant amplitude and where summation on repeated indices is assumed. In the eigenvectors basis, Eqn. (5) reads

$$\mathcal{L}[Y_s(t)]U_s(n) = Y_s(t)S_{np}U_s(p) + \mu_n(t) = -\omega_s^2 Y_s(t)U_s(n) + \mu_n(t), \quad (11)$$

The scalar product of this equation with $\mathbf{U}_{s'}$ is

$$\mathcal{L}[Y_s(t)]U_s(n)U_{s'}(n) = -\omega_s^2 Y_s(t)U_s(n)U_{s'}(n) + \mu_n(t)U_{s'}(n), \quad (12)$$

and the orthonormality of the eigenvectors basis, $U_s(n)U_{s'}(n) = \delta_{ss'}$, eventually gives

$$\frac{d^2 Y_s}{dt^2} + \Gamma \frac{dY_s}{dt} + \omega_s^2 Y_s = \mu_n(t)U_s(n) \equiv \widehat{\mu}_s(t). \quad (13)$$

Obviously, the random force is such that $\langle \widehat{\mu}_s(t) \rangle = 0$, and it is easy to show that

$$\begin{aligned} \langle \widehat{\mu}_s(t) \widehat{\mu}_{s'}(t') \rangle &= \langle \mu_n(t)U_s(n) \mu_p(t')U_{s'}(p) \rangle = \\ &= 2T\Gamma \delta(t-t') \delta_{np} U_s(n)U_{s'}(p) = 2T\Gamma \delta(t-t') \delta_{ss'}, \end{aligned} \quad (14)$$

where we have used the properties of the random force (4) and the orthonormality of the eigenvectors basis.

D. Calculation of the mean squared displacement

The physical interpretation of Eqn. (13) is very simple : each amplitude $Y_s(t)$ behaves as a damped oscillator with characteristic frequency ω_s^2 in a thermal bath at temperature T (see Ref. [29] for the description of the harmonic oscillator in a thermal bath). The corresponding MSD is

$$\langle \Delta Y_s^2(t) \rangle = \frac{2T}{\omega_s^2} \left[1 + \frac{\omega_-(s)e^{\omega_+(s)t} - \omega_+(s)e^{\omega_-(s)t}}{\omega_+(s) - \omega_-(s)} \right], \quad \omega_{\pm}(s) \equiv -\frac{\Gamma}{2} \pm \sqrt{\frac{\Gamma^2}{4} - \omega_s^2}. \quad (15)$$

This expression comes from a double averaging process. The MSD is ensemble averaged, and we average over the arbitrary time t_0 at which we take the initial conditions of the differential equation (13). The advantage of this double averaging is improving the statistics of our simulations [22].

Since the eigenmodes are uncorrelated, it is easy to reconstruct the MSD of the n -th particle [30] as a sum of the MSD of the eigenmodes amplitudes,

$$\langle \Delta y_n^2(t) \rangle = \frac{2T}{N} \left[\frac{t}{\Gamma} - \frac{1}{\Gamma^2} (1 - e^{-\Gamma t}) \right] + \frac{2}{N} \sum_{r=1}^{N-1} \cos^2 \left[\frac{r(2n-1)\pi}{2N} \right] \langle \Delta Y_r^2(t) \rangle. \quad (16)$$

The first term in the right member exhibits the contribution of the null frequency eigenmode linked to the translational invariance of the system. Note that in the sum, $r \equiv s - 1$. The equations (8), (15) and (16) provide the analytic expression for the MSD of any particle in a free boundaries chain.

This result is illustrated in Fig. 1 where we plot the MSD of the first particle ($n = 1$) and of the center particle ($n = n^*$) for an underdamped system (dotted lines) and an overdamped system as well (solid lines). Many features of these plots may be understood quite simply, because the dynamics of the particles is closely linked to those of the vibrational eigenmodes of the chain, which as shown by Eqn. (15) behave as harmonic oscillators in a thermal bath.

The first non vanishing term of the Taylor expansion of Eqn. (15) at short time shows that the MSD of each eigenmode scales as t^2 . Therefore, each term in Eqn. (16) exhibits the same behavior, which evidences that every particle in the chain undergoes the same *ballistic flight*, $\langle \Delta y^2 \rangle \propto Tt^2$, regardless on the system size N . In this short time regime, $0 < t < \tau_{corr}$ regardless of the damping, the single file correlations do not set up so that all particles are independent and therefore have equivalent behaviors (even if the crossover time slightly depends on the particle position, which will be discussed later). This regime is clearly seen in Fig. 1 for $t < 0.1$.

At large time, $t > \tau_{coll}$, the MSD of all modes with non zero frequency eventually saturate, so that the time variation of the sum in Eqn. (16) is dominated by the only contribution of the first term that corresponds to the zero frequency mode. This mode results from the translation invariance of the system and corresponds to the motion of the chain as a whole. Therefore, in this large time regime all particles have the same MSD, which corresponds to the Fickian diffusion of an effective particle with the total mass N of the chain (in our dimensionless units, the mass of a particle is 1) which undergoes normal diffusion $\langle \Delta y^2 \rangle \propto t$, with diffusivity $T/(N\Gamma)$. This is evidenced in the plots of Fig. 1, where it is seen that both particles eventually behaves in the same way. Moreover, the slopes that characterize in logarithmic scale the eventual Fickian diffusion of the chain display the two orders of magnitude expected from the chosen values of the dissipation.

Let us now focus on the intermediate time regime, $\tau_{corr} < t < \tau_{coll}$, which will be called the *correlated regime* henceforward. Roughly speaking, in this regime the dynamics of the particles is controlled by the interparticles correlations, but the time scale is not long enough for the chain to behave as an effective particle. More quantitatively, the time evolution of the MSD of any particle is due to the sequential saturation of the MSD of the eigenmodes with non zero frequency, this dynamics being dominated by the modes for which the MSD is still unsaturated at time t .

Let us first consider the small damping case, $\Gamma < \omega_r$ for all mode indices r . At time t , the eigenmodes for which the MSD remains unsaturated and scale as Tt^2 are the low frequency ones, such that $\pi/t > \omega_r$ [29]. In order to determine the number of these modes at time t , it is convenient to use the Debye approximation of the frequency spectrum (8), $\omega_r \approx r\pi/N$, because it describes accurately the low frequency spectrum. In this framework, the index of the last unsaturated mode $R(t)$ at time t is thus $R(t) \approx N/t$.

For a mode of index r with $1 \leq r \leq R(t)$, we get

$$\langle \Delta Y_r^2(t) \rangle = \frac{2T}{\omega_r^2} (1 - e^{-\Gamma t/2} \cos \omega_r t) \approx Tt^2. \quad (17)$$

In contrast, the contribution of a mode of index $r > R(t)$ is $\langle \Delta Y_r^2(t) \rangle = T/\omega_r^2$ and does not depends on time. Therefore, the MSD of the n th-particle reads

$$\langle \Delta y_n^2(t) \rangle = \frac{2TC(n, R(t))}{N} t^2 + \frac{2T}{N} \sum_{r=R(t)+1}^{N-1} \left(\frac{\cos r\alpha_n}{2 \sin \frac{r\pi}{2N}} \right)^2, \quad (18)$$

where $\alpha_n \equiv (2n - 1)\pi/(2N)$, and where

$$C(n, R(t)) = 1 + \sum_{r=1}^{R(t)} \cos^2 r\alpha_n = 1 + \frac{R(t)}{2} + \frac{\cos(R(t) + 1)\alpha_n \sin R(t)\alpha_n}{2 \sin \alpha_n}, \quad (19)$$

where we have used Ref. [28] to get the last expression.

The time variation of the MSD of the n -th particle is dominated by the first term in the right member of Eqn. (18). Note that in the coefficient $C(n, R(t))$, the relative weight of each mode is taken into account through the terms containing α_n . Therefore, the index $R(t)$ of the highest frequency unsaturated mode at time t actually depends on the particle position n . This point will be discussed more in details at the end of this section. Nevertheless, regardless of the particle index n , the particle MSD scales as $(T/N)t^2R(t) = Tt$ in the correlated regime, for all N [31]. This is a seemingly Fickian diffusion, but with a diffusivity which is neither the free particle diffusivity T/Γ (in our dimensionless units) nor the effective diffusivity $[T/(N\Gamma)]$ observed when eventually the chain diffuses as a whole.

In the opposite regime of large damping, $\Gamma > \omega_r$ for all mode index r , the frequencies in Eqn. (15) are $\omega_- \approx -\Gamma$ and $\omega_+ \approx -\omega_r^2/\Gamma$, such that $|\omega_-| > |\omega_+|$ [29]. At a given time t , the MSD of the modes such that $\omega_+ < 1/t$ are not saturated and behave as

$$\langle \Delta Y_s^2(t) \rangle = \frac{2T}{\omega_s^2} (1 - e^{\omega_+ t}) \approx \frac{2Tt}{\Gamma}. \quad (20)$$

Proceeding as before, the MSD of the n -th particle now reads

$$\langle \Delta y_n^2(t) \rangle = \frac{2TC(n, R(t))}{N\Gamma} t + \frac{2T}{N} \sum_{r=R(t)+1}^{N-1} \left(\frac{\cos r\alpha_n}{2 \sin \frac{r\pi}{2N}} \right)^2, \quad (21)$$

where $R(t) \approx N\sqrt{\Gamma}/(\pi\sqrt{t})$. Therefore the particles MSD in the large damping case scales as $\langle \Delta y_n^2(t) \rangle \approx [4Tt/(N\Gamma)]R(t) \approx 4T\sqrt{t}/(\pi\sqrt{\Gamma})$, which evidences the peculiar SFD scaling $\langle \Delta y_n^2(t) \rangle \propto \sqrt{t}$.

E. Dependence of the MSD on the particle position

Let us now focus on the dependence of the n -th particle MSD upon the index n . At short and long times the MSD are identical for all particles since at short time the particles are all independent and at long time all particles undergo the same collective diffusion. In

contrast, the MSD depend on the particle position along the chain in the correlated regime. This is specific to the chain with free boundaries.

Two effects have to be considered. A first glance on Fig. 1 evidences that the amplitude of the MSD of the free end particle is much higher than that of the center particle in the correlated regime. This is the main *free ends effect*. A more subtle one concerns the crossover times which characterize the duration of the correlated regime. They slightly increase from the center particle to the extremities. The origin of these two effects is the same. Indeed, for a finite chain with free ends, the contribution of each mode to the particle displacement differs from one particle to another, which induces an explicit dependence on the particle index n of the coefficient $C(n, R(t))$ in Eqn. (19) through α_n .

In order to understand the effects introduced by $C(n, R(t))$, let us compare the particle at the free end ($n = 1$) to the center particle ($n = (N + 1)/2 \equiv n^*$, assuming for definiteness an odd number of particles N). In Fig. 2, we plot $C(1, R)$ and $C(n^*, R)$ as a function of R , for $1 \leq R \leq N - 1$. The eigenmodes amplitudes $U_r(n)$ as a function of their index r are plotted for the particle $n = 1$ and $n = n^*$ in the inset (see Eqn. (9); we recall that $r \equiv s - 1$).

For $n = n^*$, half of the eigenmodes have a vanishing amplitude and hence do not contribute to the particle MSD, whereas the other half of the modes have the same amplitude. Very different behavior may be observed for the free ends ($n = 1$ or $n = N$). In this case, all the modes contribute even if the amplitudes of the highest frequency modes are much smaller than those of the low frequency modes. This explains the fluctuation enhancement by a factor roughly equal to 2 for the free ends with respect to the center particle one observed in Fig. 1. Note that this fluctuations enhancement is evidenced regardless of the damping constant, and depends weakly on the system size since the vanishing of half modes for the center particle only results from the projection of the center particle displacement on the eigenmodes.

Another consequence of these different eigenmodes behaviors reflects in the plots of $C(n, R)$. As shown in Fig. 2, for the center particle $C(n^*, R)$ increases as R/N whereas for the first particle $C(1, R)$ increases with a larger slope, roughly $2R/N$, then saturates for $R \geq N/2$. This indicates that the dynamics of the extremities are essentially controlled by the low frequencies modes in contrary of the center particle case for which the whole frequency spectrum is involved. As a consequence, the crossover times τ_{corr} and τ_{coll} for the correlated regime depend on the particle position.

The crossover time τ_{corr} is the time at which the process of sequential saturation described by Eqns. (18) and (21) begins. For an underdamped system, it corresponds to the time for which a first mode leaves its ballistic flight. The crossover time is then roughly given by $\tau_{corr} \sim \pi/\omega_{N-1} = \pi/2$. This is what happens for the center particle. On another hand, when $C(n \neq n^*, R)$ saturates for a lower frequency $\omega_{sat}(n) < \pi/\omega_{N-1}$, the sequential saturation takes place at $\tau_{corr} \sim \pi/\omega_{sat}$. Thus for the particle $n = 1$, $\tau_{corr}(n = 1) \sim 2\tau_{corr}(n = n^*)$. This effect is illustrated in Fig. 3 which displays $\langle \Delta y_n^2(t) \rangle / t^2$ as a function of time t for several damping coefficients. These ratios, equal to 1 at very short time regardless of the damping decrease as soon as the ballistic regime is left, at a time $t \sim \tau_{corr}$. For the underdamped system, we can see that $\langle \Delta y_1^2(t) \rangle / t^2$ decreases at a time twice higher than $\langle \Delta y_{n^*}^2(t) \rangle / t^2$. In contrast, for overdamped systems the ballistic regime is left at $\tau_{corr} \sim 2/\Gamma$ whatever the particle position.

The crossover τ_{coll} which ends the correlated regime also depends on the particle position. For very small damping, the collective regime following the SFD regime is the ballistic regime of the translational mode and it takes place as soon as $\langle \Delta y_n^2(t) \rangle$ is dominated by the quadratic time variation of the zero frequency mode while the MSD of the other modes are all saturated. Thus, according to Eqn. (18) $\tau_{coll}(n)$ may be estimated by

$$\tau_{coll}(n) \sim \sqrt{2 \sum_{r=1}^{N-1} \frac{\cos^2(r\alpha_n)}{\omega_r^2}} \sim N \sqrt{\frac{2}{\pi^2} \sum_{r=1}^{N-1} \frac{\cos^2(r\alpha_n)}{r^2}}, \quad (22)$$

where we have used the Debye approximation.

For larger damping, the collective regime following the SFD regime is the diffusive regime of the translational mode and it takes place as soon as $\langle \Delta y_n^2(t) \rangle$ is dominated by the linear time variation of the zero frequency mode while the MSD of the other modes are all saturated. Thus, according to Eqn. (21) $\tau_{coll}(n)$ may be estimated by

$$\tau_{coll}(n) \sim \Gamma \sum_{r=1}^{N-1} \frac{\cos^2(r\alpha_n)}{\omega_r^2} \sim N^2 \Gamma \frac{1}{\pi^2} \sum_{r=1}^{N-1} \frac{\cos^2(r\alpha_n)}{r^2}, \quad (23)$$

Therefore, if all the modes had the same weight, τ_{coll} would vary as N for underdamped systems and as $N^2\Gamma$ for overdamped systems. However, the crossover time τ_{coll} slightly varies with the particle position n through the sums in (22) and (23).

III. COMPARISON WITH NUMERICAL SIMULATIONS

In this section, our theoretical analysis is compared to numerical simulations. The simulation is based on the Gillespie algorithm [32, 33] that allows a consistent time discretization of the Langevin equation [22]. We restrict our simulations to a low temperature, $T < 1$ in our units since the unit energy is the potential energy between nearest neighbors. In all simulations we take $T = 10^{-3}$. In this way, we ensure thermodynamic stability of the particles chain. We vary the damping Γ from the underdamped regime ($\Gamma = 4 \cdot 10^{-3}$) to the overdamped regime ($\Gamma = 3$). The size of the system is chosen between $N = 17$ and $N = 235$ in order to explore the limitation of our model with N .

In Fig. 4 we plot the MSD of the extremities and of the center particle in the chain as a function of time, for a very underdamped system [Fig. 4 (a), $\Gamma = 4 \cdot 10^{-3}$] and an overdamped system [Fig. 4 (b), $\Gamma = 3$]. Together with the simulations data, we display the theoretical MSD deduced from Eqns. (18) and. (21). The simulation data and the calculations are in perfect agreement without any free parameter. Notice also the excellent agreement for both damping between the MSD of the center particle and the black solid line which displays the MSD of a particle embedded in a periodic or infinite chain, even for the rather moderate chain length ($N = 33$). This effect comes from the linear dependence of $C(n^*, R)$ with R which implies a MSD for the center particle that scales as Tt/π for low damping and $2Tt^{1/2}/(\pi\Gamma^{1/2})$ for large damping. These scalings are exactly those of a particle embedded in a periodic or infinite chain [22]. Therefore, we will take hereafter the MSD of the central particle as reference in order to directly exhibit the specificities introduced by the chain with free extremities.

A. Fluctuations enhancement in the correlated regime

In the insets of Fig. 4 we plot the MSD ratio $\langle \Delta y_N^2(t) \rangle / \langle \Delta y_*^2(t) \rangle$ as a function of time, for a small damping [Fig. 4-(a)] and a large damping [Fig. 4-(b)]. As expected, the MSD of a particle at one extremity is about twice as large as the MSD of the center particle, regardless of the damping even if it differs by three orders of magnitude between the top and bottom plot. The maximum value of the MSD ratio is also seen to be roughly independent on the

system size.

This fluctuations enhancement is not restricted to the first and last particle in the chain. In Fig. 5 we display the ratio $\langle \Delta y_i^2(t_0) \rangle / \langle \Delta y_*^2(t_0) \rangle$ as a function of the particle index i , at several times t_i that range in the correlated regime, for the simulations of Fig. 4. To be specific, the times t_i are set at 10%, 50% and 90% of the duration of the correlated regime. The analytical expression of the MSD ratios, derived from Eqn. (16), is in very good agreement with the simulations data. As times goes by, the particles that undergo a significant fluctuations enhancement (more than a 50% increase, say) are close to the free ends, roughly five when 90% of the duration of the correlated regime has elapsed.

B. Crossover times

The bell shaped curve $\langle \Delta y_N^2(t) \rangle / \langle \Delta y_*^2(t) \rangle$ displayed in Fig. 5 begins to increase monotonically from 1 at the crossover time $\tau_{corr}(n^*)$ until reaching a plateau at time $\tau_{corr}(1)$. The main feature of this increase of the MSD ratio is to be independent of N as explained in Sec. II E. Its duration, which reflects the delay of the particles at the ends with respect to the center particle to reach the correlated regime is also in agreement with our analysis.

In contrast with the initial increase, the decrease of the plateau toward its eventual limiting value (1, since eventually all particles diffuses in the same way) strongly depends on the system size N and on the damping constant Γ . The ratio $\langle \Delta y_N^2(t) \rangle / \langle \Delta y_*^2(t) \rangle$ begins to decrease monotonically at the crossover time $\tau_{coll}(n^*)$ and reaches its asymptotic value 1 at $\tau_{coll}(1)$. For underdamped systems [Fig. 5–(a)], the collective time τ_{coll} scales as N and the delay between $\tau_{coll}(n^*)$ and $\tau_{coll}(1)$ is around 2 as expected. For overdamped systems [Fig. 5–(b)], the collective time τ_{coll} scales as ΓN^2 and the delay between $\tau_{coll}(1) \approx 4\tau_{coll}(n^*)$ as expected.

A quantitative test of our analysis is undertaken in Fig. 7, where we plot the crossover time τ_{coll} , defined as the time at which the ratio $\langle \Delta y_N^2(t) \rangle / \langle \Delta y_*^2(t) \rangle$ provided by the simulations data leaves its plateau, as a function of the chain length N for a large range of chains length ($17 \leq N \leq 255$) and damping constants ($0.004 \leq \Gamma \leq 3$). We then compare these estimates of τ_{coll} to our estimates. In the low damping case [Fig. 7–(a), $\Gamma \leq 0.04$] the observed crossover time is indeed independent on Γ and proportional to the chain length N . In the large damping case [Fig. 7–(b), $0.04 \leq \Gamma$] the observed crossover time scales as N^2 and is

proportional to Γ . Our analysis of the crossover time τ_{coll} is thus fully validated.

The case $\Gamma = 0.04$, interestingly, is in rather good agreement with the small damping prediction for small chains ($N = 17, 33$ and 65) and in much better agreement with the large damping prediction for large chains ($N = 127, 191$ and 255). It may thus be considered as the actual limit between the low damping and the large damping dynamics.

IV. CONCLUSION

We study the transport of a chain of particles with free ends, embedded in a thermal bath and in confined geometries that forbids any crossing of the particles. We describe the displacement of each particle as a superposition of contributions of the vibration eigenmodes of the chain. The MSD of the particle is then simply the relevant weighted sum of the MSD of these eigenmodes. This model is conceptually and technically very simple, and it is neither restricted to the thermodynamic limit (infinite systems with finite density) nor to overdamped systems. We obtain a formula for the MSD of any individual particle as a function of the temperature T of the thermal bath, which is found to successfully predict the thermal fluctuations at all time.

Each particle undergoes a short-time motion that is free diffusion with diffusivity T/Γ (in our dimensionless units, with Γ the damping constant), and eventually the long-time motion of the N particles chain as a whole is a Fickian diffusion with diffusivity $T/(N\Gamma)$. Whatever the damping, we identify between these two time scales an *intermediate correlated regime*. This regime is dominated by the interparticles correlations. At large damping, the MSD evidences the typical SFD behavior, with a time dependence scaling as $t^{1/2}$. At small damping, the correlated regime is not described by the SFD scaling, but rather by a diffusion-like behavior, with the MSD time dependence in t , but with a diffusivity T/π which is neither the individual particle diffusivity nor the diffusivity of the chain as a whole.

These various regimes are relevant for every particles, but most importantly the amplitude of the fluctuations and the crossover times depend upon the particle position in the chain with free ends. The fluctuations of the particles at each extremity are larger by a factor two than the fluctuations of the center particle. This effect is observed whatever the damping, and the duration of this MSD enhancement increases with the damping and with the chain length, as N for low damping and as ΓN^2 for high damping.

This model could be useful to analyze the diffusion of constrained chains. For instance, it could allow the analysis of macromolecule transport through thin channels in which any folding of the macromolecule should be ruled out. Such a configuration is relevant to macromolecule transport through cell membranes, through zeolites or through carbon nanotubes [2–6]. A chain of identical particles is admittedly a rather crude model of a macromolecule, since it does not take into account the internal degrees of freedom of the individual molecules. Nevertheless, it should be relevant if the monomers are small enough for their internal degrees of freedom to be of small consequences on their thermal transport. We also remark that our calculations are easily expanded to more general chain models, as long as the mass and spring constants distributions are known. Let us add that our model does not take into account macromolecule folding, but is not invalidated by transverse fluctuations, since those latter are decoupled, in the linear approximation, from the longitudinal motions [34].

The MSD measurements are useful to characterize the dynamics properties of a system submitted to a thermal bath. In this perspective, the understanding of the enhancement of thermal fluctuations near the ends of the chain offered by this model could be an interesting opportunity, of practical significance for actual measurements. For instance, if we consider an experiment in which one molecule is tagged with a fluorescent marker, our study evidences that the position of the marker along the macromolecule has to be known precisely if one wants to measure the actual transport coefficient of the macromolecule in a confined geometry from the observed fluctuations of the tagged molecule. We note that the MSD may not be a reliable estimator of particle diffusivity [35, 36], but it is nevertheless interesting to evidence a potential systematic error.

-
- [1] A.L. Hodgkin and R.D. Keynes, “The potassium permeability of a giant nerve fibre,” *J. Physiol.* **128**, 61–88 (1955).
 - [2] Paul C. Bressloff and Jay M. Newby, “Stochastic models of intracellular transport,” *Rev. Mod. Phys.* **85**, 135 (2013).
 - [3] V. Gupta, S. S. Nivarthi, A. V. McCormick, and H. T. Davis, “Evidence for single file diffusion of ethane in the molecular sieve $\text{AlPO}_4\text{-5}$,” *Chem. Phys. Lett.* **247**, 596–600 (1995).

- [4] T. Chou and L. Detlef, “Entropy-driven pumping in zeolites and biological channels,” *Phys. Rev. Lett.* **82**, 3552 (1999).
- [5] P. Demontis, G. Stara, and G.B. Suffritti, “Dynamical behavior of one-dimensional water molecule chains in zeolites: Nanosecond time-scale molecular dynamics simulations of biki-taite,” *J. Chem. Phys.* **120**, 9233 (2004).
- [6] P. Hänggi and F. Marchesoni, “Artificial brownian motors : Controlling transport on the nanoscale,” *Rev. Mod. Phys.* **81**, 387 (2009).
- [7] S. Seidelin, J. Chiaverini, R. Reichle, J. J. Bollinger, D. Leibfried, J. Britton, J. H. Wesenberg, R. B. Blakestad, R. J. Epstein, D. B. Hume, W. M. Itano, J. D. Jost, C. Langer, R. Ozeri, N. Shiga, and D. J. Wineland, “Microfabricated surface-electrode ion trap for scalable quantum information processing,” *Phys. Rev. Lett.* **96**, 253003 (2006).
- [8] R. Besseling, R. Niggebrugge, and P.H. Kes, “Transport properties of vortices in easy flow channels: A frenkel-kontorova study,” *Phys. Rev. Lett.* **82**, 3144 (1999).
- [9] N. Kokubo, R. Besseling, and P.H. Kes, “Dynamic ordering and frustration of confined vortex rows studied by mode-locking experiments,” *Phys. Rev. B* **69**, 064504 (2004).
- [10] N. Kokubo, T. G. Sorop, R. Besseling, and P. H. Kes, “Vortex-slip transitions in superconducting a -nbge mesoscopic channels,” *Phys. Rev. B* **73**, 224514 (2006).
- [11] Bianxiao Cui, H. Diamant, and Binhua Lin, “Screened hydrodynamic interaction in a narrow channel,” *Phys. Rev. Lett.* **89**, 188302 (2002).
- [12] Binhua Lin, Bianxiao Cui, Ji-Hwan Lee, and J. Yu, “Hydrodynamic coupling in diffusion of quasi-one-dimensional brownian particles,” *EPL* **57**, 724 (2002).
- [13] Binhua Lin, Mati Meron, Bianxiao Cui, Stuart A. Rice, and H. Diamant, “From random walk to single-file diffusion,” *Phys. Rev. Lett.* **94**, 216001 (2005).
- [14] M. Köppl, P. Henseler, A. Erbe, P. Nielaba, and P. Leiderer, “Layer reduction in driven 2d-colloidal systems through microchannels,” *Phys. Rev. Lett.* **97**, 208302 (2006).
- [15] P. Henseler, A. Erbe, M. Köppl, P. Leiderer, and P. Nielaba, “Density reduction and diffusion in driven two-dimensional colloidal systems through microchannels,” *Phys. Rev. E* **81**, 041402 (2010).
- [16] T. E. Harris, “Diffusion with ”collisions” between particles,” *J. Appl. Prob.* **2**, 323–338 (1965).
- [17] David G. Levitt, “Dynamics of a single file pore : non-fickian behavior,” *Phys. Rev. A* **8**, 3050 (1973).

- [18] Henk van Beijeren, K. W. Kehr, and R. Kutner, “Diffusion in concentrated lattice gases. III. tracer diffusion on a one-dimensional lattice.” *Phys. Rev. B* **28**, 5711 (1983).
- [19] R. Arratia, “The motion of a tagged particle in the simple symmetric exclusion system on Z^1 ,” *Ann. Prob.* **11**, 362–373 (1983).
- [20] M. Kollmann, “Single-file diffusion of atomic and colloidal systems: Asymptotic laws,” *Phys. Rev. Lett.* **90**, 180602 (2003).
- [21] B.U. Felderhof, “Fluctuation theory of single-file diffusion,” *J. Chem. Phys.* **131**, 064504 (2009).
- [22] J.-B. Delfau, C. Coste, and M. Saint Jean, “Single file diffusion of particles with long-ranged interactions: Damping and finite size effects,” *Phys. Rev. E* **84**, 011101 (2011).
- [23] P. Hänggi and P. Jung, “Colored noise in dynamical systems,” *Adv. Chem. Phys.* **89**, 239 (1995).
- [24] O. Yu. Sliusarenko and A. V. Chechkin, “Kinetic equations for non-markovian gaussian processes in linear multidimensional systems,” *Ukr. J. Phys.* **52**, 1193 (2007).
- [25] O. Yu. Sliusarenko, “Generalized fokker-planck equation and its solution for linear non-markovian gaussian systems,” *Cond. Mat. Phys.* **14**, 23002 (2011).
- [26] L. Brillouin and M. Parodi, *Propagation des ondes dans les milieux périodiques* (Masson, Paris, 1956).
- [27] Wen-Chyuan Yueh, “Eigenvalues of several tridiagonal matrices,” *Applied Mathematics E-notes* **5**, 66 (2005).
- [28] I.S. Gradshteyn and I.M. Ryzhik, *Table of Integrals, Series, and Products* (Academic Press, 2007).
- [29] S. Chandrasekhar, “Stochastic problems in physics and astronomy,” *Rev. Mod. Phys.* **15**, 2 (1943).
- [30] J.-B. Delfau, C. Coste, and M. Saint Jean, “Single file diffusion of particles in a box : Transient behaviors,” *Phys. Rev. E* **85**, 061111 (2012).
- [31] Let us add a word of caution. In this discussion, it is implicitly assumed that the system is large enough, in order that $R(t) < 1$. The relevant order of magnitude for the system size N is the double of the typical extension of the enhanced fluctuations at the free ends. From Fig. 5, it means $N > 20$, say.
- [32] Daniel T. Gillespie, “Exact numerical simulation of the ornstein-uhlenbeck process and its

- integral,” *Phys. Rev. E* **54**, 2084 (1996).
- [33] Daniel T. Gillespie, “The mathematics of brownian motion and johnson noise,” *Am. J. Phys.* **64**, 225 (1996).
- [34] J.-B. Delfau, C. Coste, and M. Saint Jean, “Transverse single-file-diffusion near the zigzag transition,” *Phys. Rev. E* **87**, 032163 (2013).
- [35] X. Michalet and A. J. Berglund, “Optimal diffusion coefficients estimation in single-particle tracking,” *Phys. Rev. E* , 061916 (2012).
- [36] C. L. Vestergaard, P. C. Blainey, and H. Flyvbjerg, “Optimal estimation of diffusion coefficients from single particle trajectories,” *Phys. Rev. E* **89**, 022726 (2014).

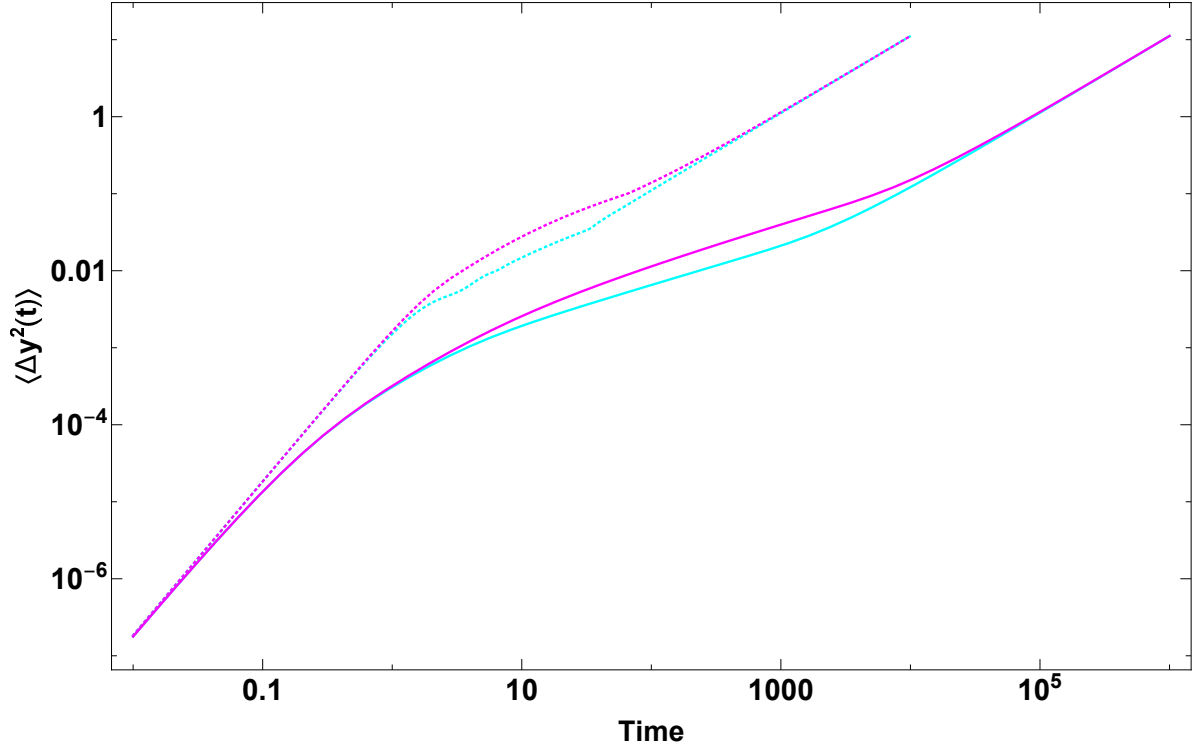


FIG. 1. (Color online) Mean squared displacement $\langle \Delta y_n^2(t) \rangle$ (logarithmic scale) as a function of time (logarithmic scale), in dimensionless units, for a system of $N = 33$ particles, from the formula given in Eqn. (16). Dotted lines underdamped system, $\Gamma = 0.1$, solid lines overdamped system, $\Gamma = 10$. Magenta lines first particle, $n = 1$, cyan lines center particle, $n = n^* = 17$.

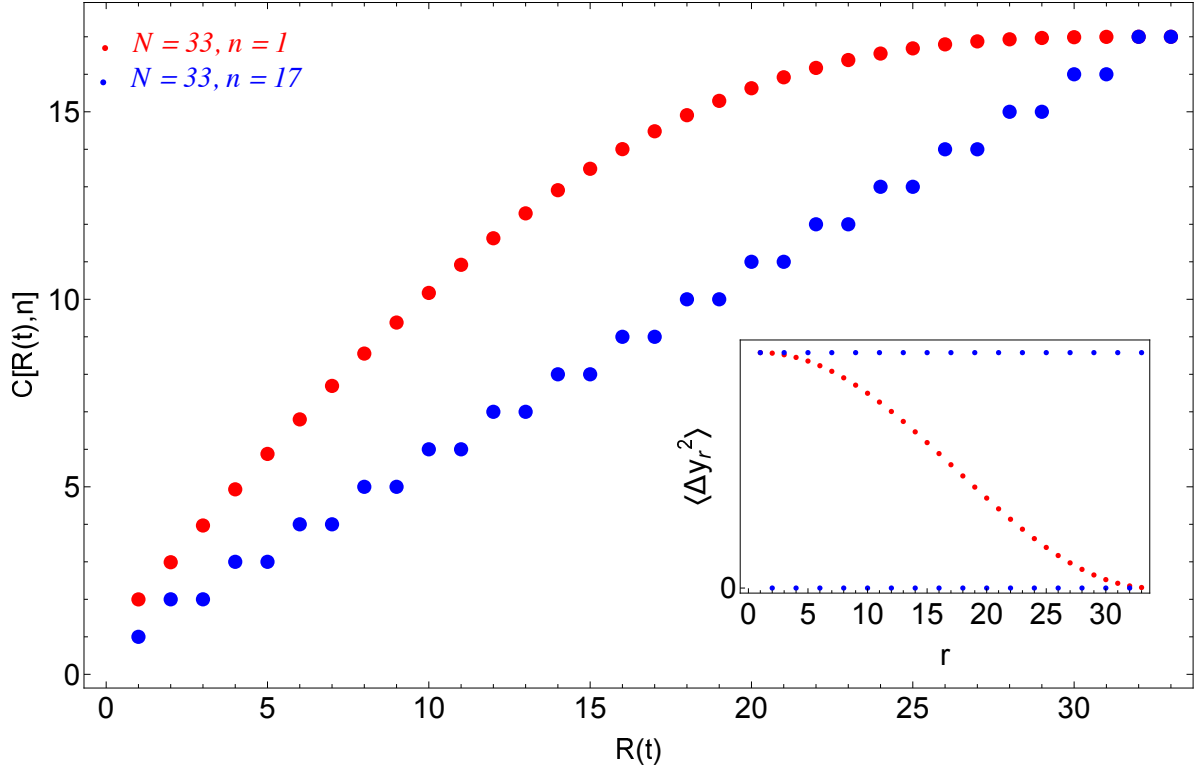


FIG. 2. (Color online) Plot of the coefficient $C[n, R(t)]$ [see Eqn. (19)] as a function of $R(t)$ for a particle at a free end ($n = 1$, red) and a particle at the center ($n = n^* = 17$, blue) in a chain of $N = 33$ particles. In the inset, we display the squared amplitude $U_r(n)^2$ for the same particles, with the same color code, as a function of the mode index r .

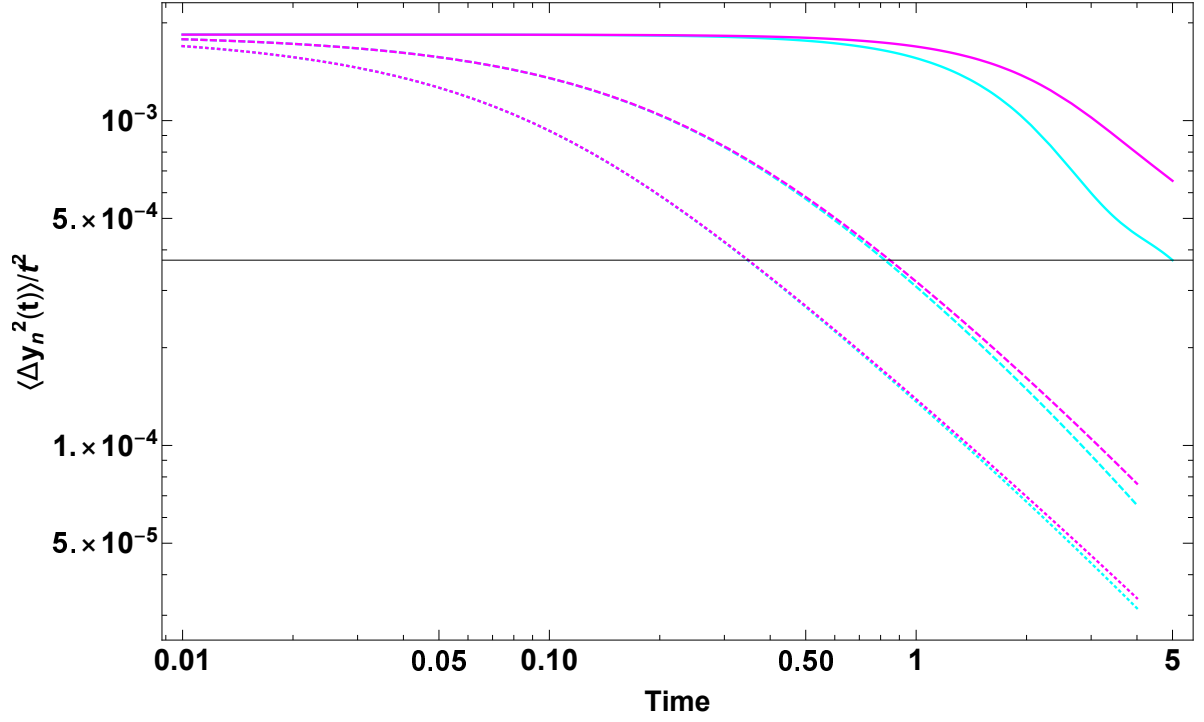


FIG. 3. (Color online) Plot of $\langle \Delta y_n^2(t) \rangle / t^2$ (logarithmic scale) as a function of time t (logarithmic scale) for a particle at a free end ($n = 1$, magenta) and a particle at the center ($n = n^*$, cyan) in a chain of $N = 33$ particles. The damping constants are $\Gamma = 0.01$ (solid lines), $\Gamma = 10$ (dashed lines) and $\Gamma = 25$ (dotted lines).

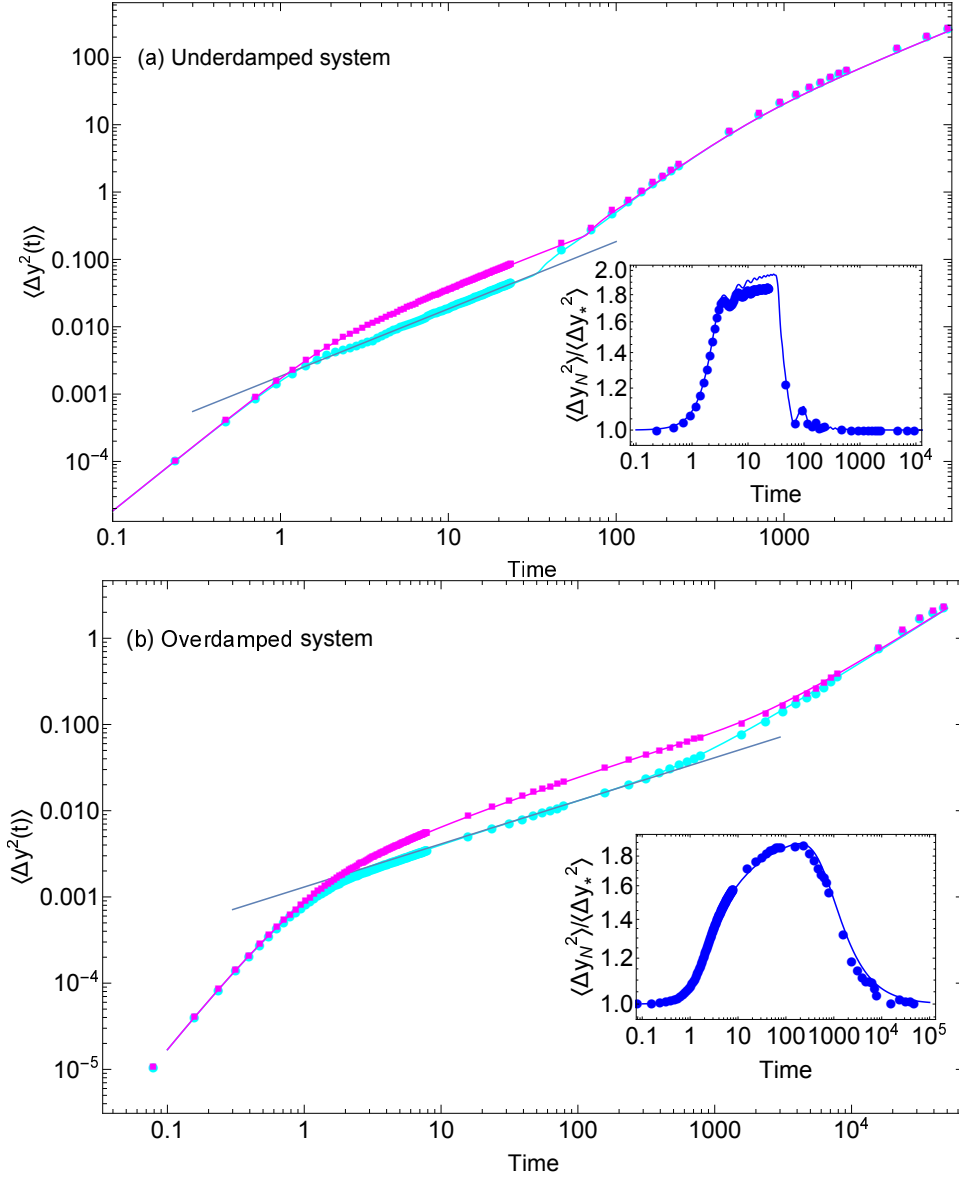


FIG. 4. (Color online) Mean squared displacement $\langle \Delta y^2(t) \rangle$ (logarithmic scale) as a function of time (logarithmic scale), in dimensionless units, for a system of $N = 33$ particles. (a) : underdamped system, $\Gamma = 4 \cdot 10^{-3}$. (b) : overdamped system, $\Gamma = 3$. Note that the times scales are different for (a) and (b). Cyan disks : MSD of the center particle n^* . Magenta squares : MSD of the particles at the extremities, $n = 1$ or $n = N$. The points are obtained from numerical simulations, the solid line of the same color is the relevant analytic expression, Eqn. (16). The black solid line is the analytical expression for the MSD in the thermodynamic limit, for the relevant damping coefficient (slope 1 for underdamped case, slope 1/2 for overdamped case; see text for details). In the insets, we plot the ratio $\langle \Delta y_N^2(t) \rangle / \langle \Delta y_*^2(t) \rangle$ (logarithmic scale) as a function of time (logarithmic scale). The points are numerical simulations data, the solid line is the analytic expression.

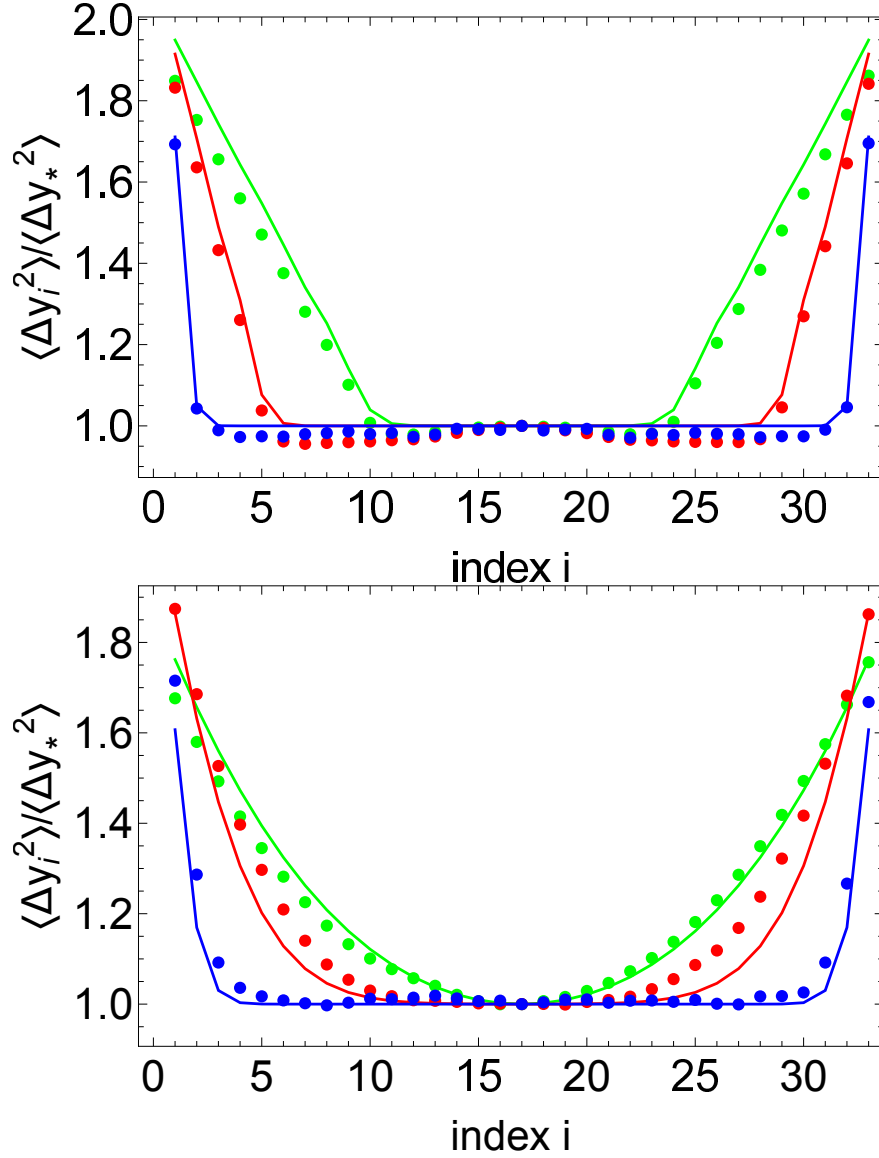


FIG. 5. (Color online) Ratio $\langle \Delta y_i^2(t_0) \rangle / \langle \Delta y_*^2(t_0) \rangle$ as a function of the particle index i for a system of $N = 33$ particles and a fixed time t_0 in the intermediate (correlated) time regime. Top : underdamped system, $\Gamma = 4 \cdot 10^{-3}$ and $t_0 = 7$. Bottom : overdamped system, $\Gamma = 3$ and $t_0 = 80$. Dots are simulations data, solid lines are calculated from Eqn. (16)

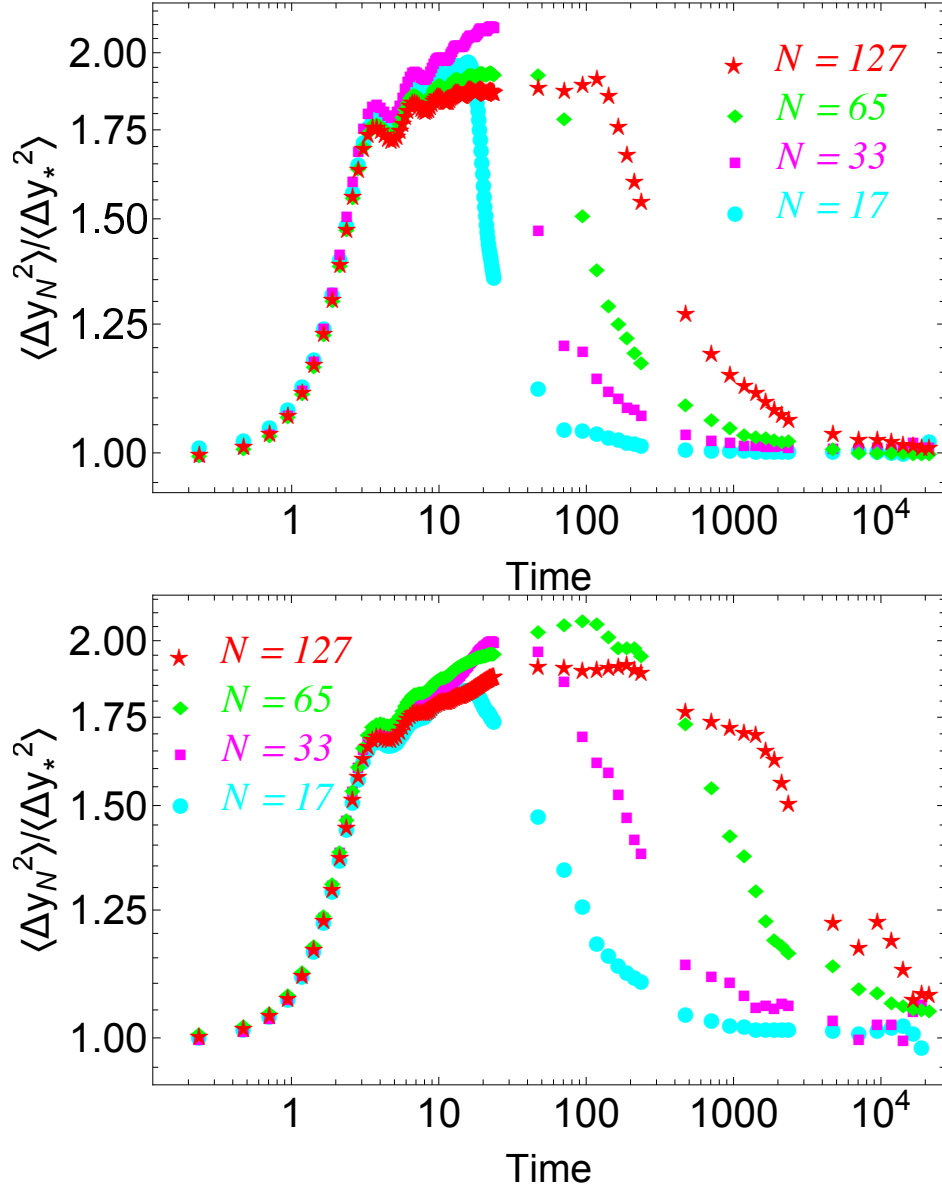


FIG. 6. (Color online). Ratio $\langle \Delta y_N^2(t) \rangle / \langle \Delta y_*^2(t) \rangle$ (logarithmic scale) as a function of time (logarithmic scale, dimensionless units) for several chains, and $\Gamma = 0.04$ (top) or $\Gamma = 0.4$ (bottom).

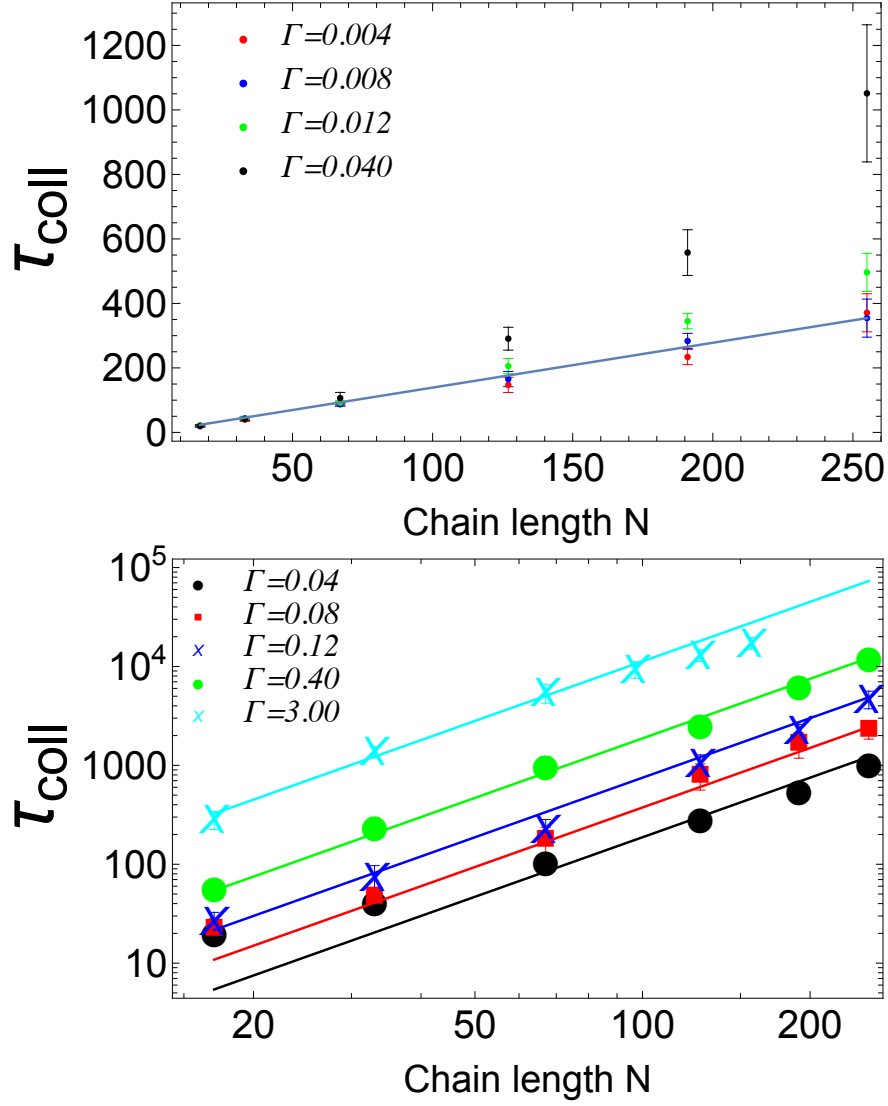


FIG. 7. (Color online). Top : Dimensionless crossover time τ_{coll} as a function of the chain length N (linear scales on both axes) for several values of Γ . The solid black line is the low damping estimate $\tau_{coll} = N$. Bottom : Dimensionless crossover time τ_{coll} as a function of the chain length N , in logarithmic scales, for several values of Γ . The solid lines with the same colors as the relevant simulations data are the high damping estimate $\tau_{coll} = N^2\Gamma$.